Dual Band GNSS Antenna With High Back Lobe Suppression

Sachit Varma, Stefano Caizzone
Institute of Communication & Navigation, German Aerospace Center (DLR), Oberpfaffenhofen, Germany
sachit.varma@dlr.de; stefano.caizzone@dlr.de

***Abstract*—This paper presents the study of a novel design of a miniaturized GNSS antenna for E5a and E1 bands (i.e. at the central operating frequencies of 1.176 and 1.575 GHz) with high gain and very low back lobe for multipath reduction in high end static (e.g. geodesy) or dynamic (e.g. UAV) environments. The antenna itself is 56 mm in diameter and has a vertically stacked appurtenance of approximately 160 mm diameter that forces the cancellation of electromagnetic fields underneath the ground plane, thereby drastically improving the cross polarization discrimination and allowing for multipath suppression in both bands of operation.**

***Index Terms*—antennas, cross polarization, GNSS, multipath, back lobe, interference.**

I. INTRODUCTION

The massive growth of GNSS (Global Navigation Satellite Systems) has been one of the biggest scientific and technological achievements and has proven to be a global game changer. What started in the early years as an elemental development for providing the position, velocity and time to support navigation and connectivity, has now evolved into a backbone technology for a plethora of innovative applications. Agriculture, racing, mountain sports, guidance of the visually impaired, archaeology, geo-fencing, skydiving, atmospheric sensing etc. are just a few of the areas that have immensely benefitted due to the outreach of GNSS [1], [2]. The variables in the picture are always the same, but making their use in life improving applications is what made GNSS a success.

Like all other technologies based on electromagnetics, the robust and error-free use of GNSS comes with its share of challenges, namely interference, jamming and spoofing as the major ones [3]. Any GNSS antenna, due to its non-ideal radiation characteristics, has a significant amount of back lobe radiation. This gives way for any signal being reflected from the surface of the platform, on which the antenna has been installed, to be received by the antenna. This phenomenon, also known as multipath, is one of the major contributing factors to errorneous GNSS measurement. As mentioned above, all applications that involve the antenna being installed either on a large ground plane (e.g. on unmanned aerial vehicles, airplanes, satellites etc.) or on heterogeneous and irregular ground planes (e.g. on drones) pose a major problem since the antenna receives energy from its back lobe, e.g. as shown in Fig. 1.

This paper addresses this issue by proposing a structure below the radiating element, that would be able to minimize the amount of multipath received. The paper is structured with the discussion of the the major performance metrics of the GNSS antenna, specifically related to multipath rejection, in the beginning, followed by the current back lobe suppression techniques. The design of the antenna comes next followed by the proposed structure for high back lobe suppression. The simulation results are discussed next in detail, corresponding to the metrics defined, followed by some remarks to conclude the possible future work associated with this technique.

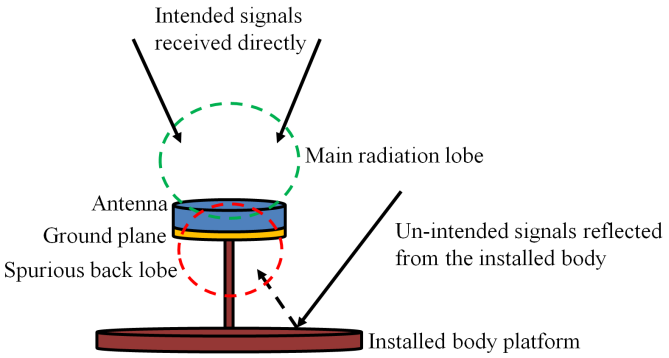

Fig. 1. Installed antenna with main and back lobe.

II. ANTENNA PERFORMANCE METRICS

A. Cross Polarization Discrimination

GNSS antennas shall be designed to radiate in RHCP (Right Hand Circularly Polarized) mode and inhibit all kinds of radiation in the LHCP (Left Hand Circularly Polarized) mode. The ratio of the former to the latter exhibits the estimate of the Cross Polarization Discrimination (XPD) over a specific elevation beam angle, and this gives us the measure of how good can the antenna receive RHCP signals and mitigate LHCP signals. Although for detection, post-correlation and mitigation of multipath in urban scenarios, dual-polarized operation, as discussed in [4] [5], is important to get a view of the direction of the desired signals and the undesired multipath signals, here in this paper the focus is on completely mitigating the undesired LHCP signals coming from the reflections below the ground plane.

B. Front-to-Back Ratio

The front-to-back ratio (FBR) of an antenna is one of the most important metrics in applications where reflection

underneath the ground plane severely hampers the received signal quality and is defined as the ratio of the maximum power gain at the antenna boresight (i.e. at 0° elevation) to the maximum power gain at its opposite end (i.e. at 180° elevation) of the intended directional antenna, where the gain at boresight refers to the RHCP signal gain and the gain at the negative side could refer to both RHCP or LHCP, whichever is higher in amplitude, as explained in [6]. In most cases, it is the LHCP component which is stronger at 180° elevation, and the technique proposed in this paper would attempt to reduce this value.

C. Axial Ratio

The axial ratio is the other important parameter of a circularly polarized antenna and is the ratio of the orthogonal polarization fields of the antenna. For a perfectly circularly polarized antenna, the orthogonal components would be equal in magnitude and 90° apart in phase giving rise to an axial ratio of 1 (or 0 dB) [7]. This ratio starts increasing in number as and when the antenna loses its perfect circular polarization tendency and starts becoming elliptic, that happens at low elevation angles for unoptimized antennas. The technique discussed in this would also attempt to improve the axial ratio of the antenna at low elevation angles.

D. Multipath Suppression Indicator (MPSI)

As extensively analyzed and discussed in [8], in an installed environment, the capability of the antenna istelf to reject multipath signals is one of the key indicators of how well the overall system would perform in the presence of multiple and distinct sources of reflection. Different multipath suppression indicators have been defined that would allow the characterization of the standalone susceptibility of the antenna to multipath for different scenarios of reflections (coming from below the antenna or from above via vertical and slanted surfaces). This important information could then be used to predict the multipath and tune the antenna beforehand.

III. BACK LOBE SUPPRESSION FUNDAMENTALS & CURRENT TECHNIQUES

In the context of reduced multipath coming from horizontal reflections from below the antenna horizon, there have been several techniques that work on mitigating this effect by targetting different electromagnetic characteristics of the antenna itself. Some of these techniques emphasize on reducing the surface waves that radiate at low elevation angles at ground plane truncations as discussed in [9], but this leads to deteriorated axial ratios since there isn't any minimum radiation amplitude at these angles anymore.

Studies on the effects of the ground plane on the antenna radiation characteristics has been studied in detail before [10] and one of the most popular techniques involving horizontal choke rings have been developed [10], [11] and [12]. This method is extremely common these days and involves choke rings that are appended horizontally to the antenna structure. These cylindrical rings act as vertical cavities for electromagnetic cancellation of fields through resonance, thus giving rise to standing waves.

As elaborately studied in [13], [14] and well known in literature, in the transmission line model treatment of a metallic cavity, the incident voltage V_{in}, load voltage V_L and reflected voltage V_r in wave form can be given by:

$$V_{in}(z,t) = V_{in}\exp[j\omega(t - z/v)]$$
$$V_r(z,t) = V_r\exp[j\omega(t + z/v)]$$
$$V_L(z,t) = V_L\exp[j\omega(t - z/v')]$$

Factoring out the time dependence and applying the conditons of voltage linearity and charge conservation at the junction, i.e. at $z = 0$, the reflection coefficient ρ would be:

$$\rho = \frac{V_r}{V_{in}} = \frac{Z_L - Z_0}{Z_L + Z_0}$$

The voltage and current as a function of transmission line length l can be given by:

$$V(l) = V_{in}\exp(-j\omega l/v) + V_r\exp(j\omega l/v)$$
$$I(l) = (V_{in}/Z_0)\exp(-j\omega l/v) - (V_r/Z_0)\exp(j\omega l/v)$$

Substituting these values for voltage and current, and for the angular frequency $\omega = 2\pi v/\lambda$, solving for the line input impedance $Z(l) = V(l)/I(l)$, we get:

$$Z(l) = Z_0\frac{Z_L + jZ_0\tan(2\pi l/\lambda)}{Z_0 + jZ_L\tan(2\pi l/\lambda)}$$

If the termination is short circuited, i.e. at $Z_L = 0$, $Z(l)$ would simply become:

$$Z(l) = jZ_0\tan(2\pi l/\lambda)$$

which gives rise to the fact that this short-circuited line would have infinite input impedance for transmission lengths equal to quarter of the operating wavelength, i.e.

$$Z(l) = \infty \text{ for, } l = (2n+1)\lambda/4, \text{where } n \in \mathbb{Z}$$

The study could be very easily made in terms of current as well that is travelling on the inner cavity walls. The analogy between this transmission line model and the cylindrical cavity is studied in [15] which shows that cavities with conductor lengths equal to quarter wavelenghts would result in the voltages (or the electromagnetic currents) balancing themselves out and causing standing waves. Horizontal choke rings with such cavities have certain drawbacks such as their bulky size and massive weight which makes installation on small body platforms impossible. The other drawback is the low gain at elevation angles beyond $\pm 20°$ mostly due to low signal strength at these angles thereby causing deteriorated positioning accuracy as studied in [16].

Another concept to reduce the surface waves in planar antennas by introducing Electronic Band Gap (EBG) structures has also been studied and developed [17]. Although the amount of back radiation is suppressed by this technique, the

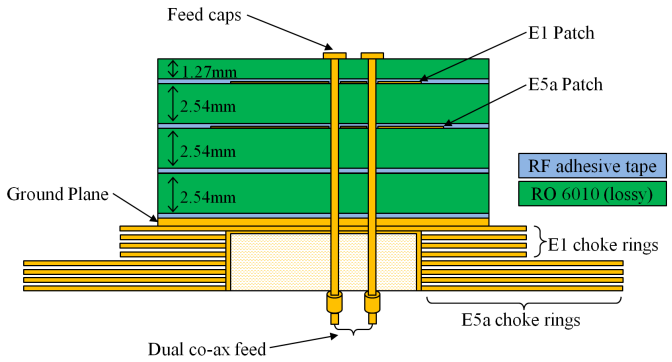

Fig. 2. Side view of stacked patch antenna with vertical choke ring cavities.

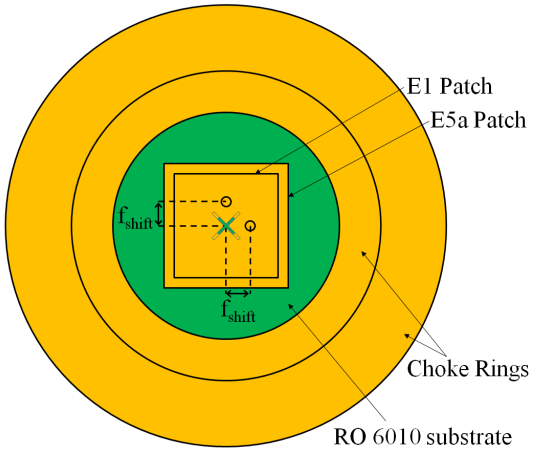

Fig. 3. Top view of stacked patch antenna with vertical choke ring cavities.

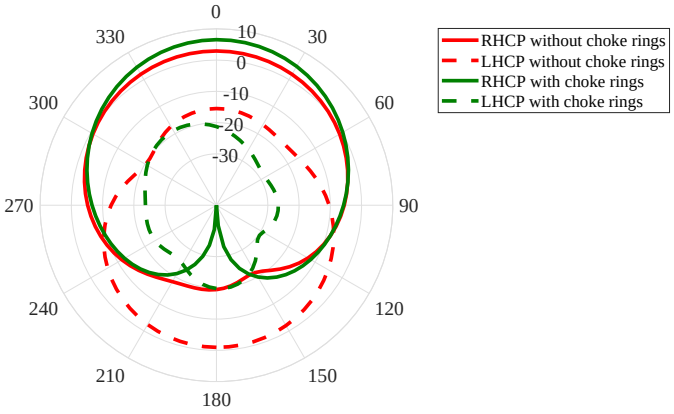

Fig. 4. Gain vs elevation at $\phi = 0°$ for E1 band.

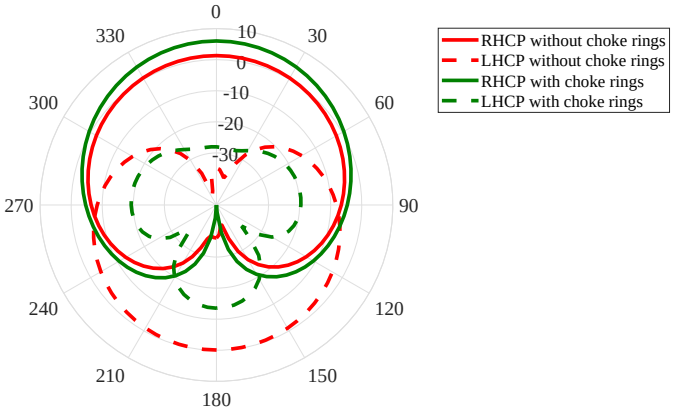

Fig. 5. Gain vs elevation at $\phi = 0°$ for E5a band.

amount of intended radiation at low elevation angles itself is reduced giving rise to poor axial ratios, as mentioned before.

As already mentioned in Section II-D about the ability of an antenna to reject multipath (from reflections at the lower and upper hemisphere of the antenna), and the correlation of this knowledge to other radiation characteristics could yield the way to characterize the multipath susceptibility and better predict the installed system performance. The measurement and analysis performed in this study clearly observed the effects of multipath on the performance of different antennas for horizontal and vertical reflections. The state-of-the-art commercial choke ring antenna did perform good but had the limitation of its big size and also the fact that its performance was mediocre in the presence of vertical reflections.

From all these studies and aforementioned implemented techniques to reduce the backward radiation from the antenna, the compromising factor is found to be either the size (or the weight) of the antenna or the reduced gain at low elevation angles (i.e. poor axial ratio). The technique mentioned in this paper will attempt to achieve the target of reducing back lobes while keeping the addendum structure minimized in size and maintaining the intended radiation performance.

IV. PROPOSED DESIGN

The design proposed in this paper consists of a series of vertical choke rings that essentially act as cavities below the circularly polarized dual band stacked patch antenna. The metallic discs in this choke structure are parallel to the ground plane, as shown in Fig. 2.

This stacked structure consists of two square patch antennas, one for each band. X-shape slots are made in the patches to improve bandwidth. The patches are fed via proximity coupling through two coaxial feedlines running through the stack. The feedlines are terminated with caps to resonate out the inductance of the line through the terminating cap induced capacitance. A readily available dielectric substrate from Rogers (RO6010) with dielectric constant (ϵ_r) $\approx$ 10.9 and thickness 2.54 mm was used along with a thin layer of an RF adhesive from Rogers (RO3010) with $\epsilon_r \approx 10.2$ and thickness 0.26 mm to join the layers.

The choke rings are placed below the ground plane in a set of notably two different diameters, one set each for E5a and the E1 band as shown in Fig. 3. Every pair of rings, or discs, acts as a parallel cavity which is approximately $\lambda/4$ in length (i.e. $\approx$ 43 mm for E1 and $\approx$ 63.5 mm for E5a) from the central metallic pillar. The exact length was slightly optimized for the entire design target to be achieved. The

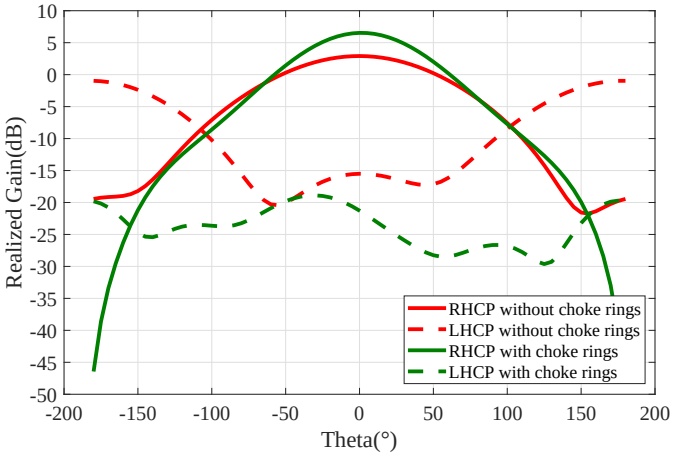

Fig. 6. Cross polarization discrimination at E1 band.

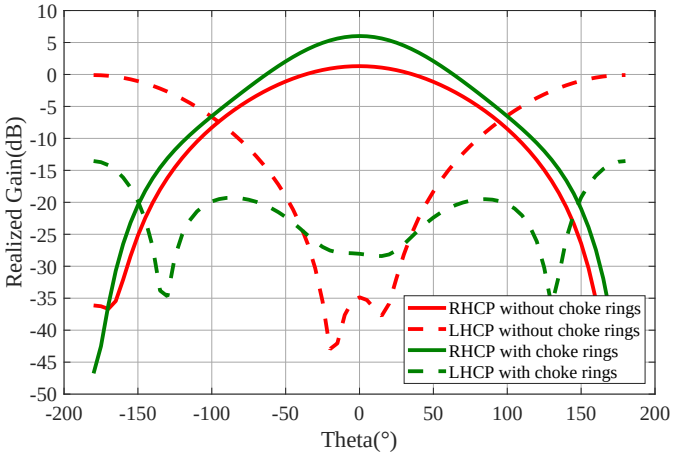

Fig. 7. Cross polarization discrimination at E5a band.

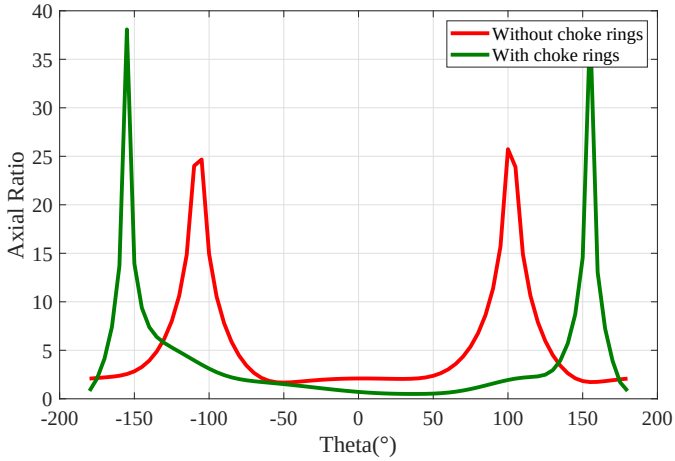

Fig. 8. Axial Ratio at E1 band.

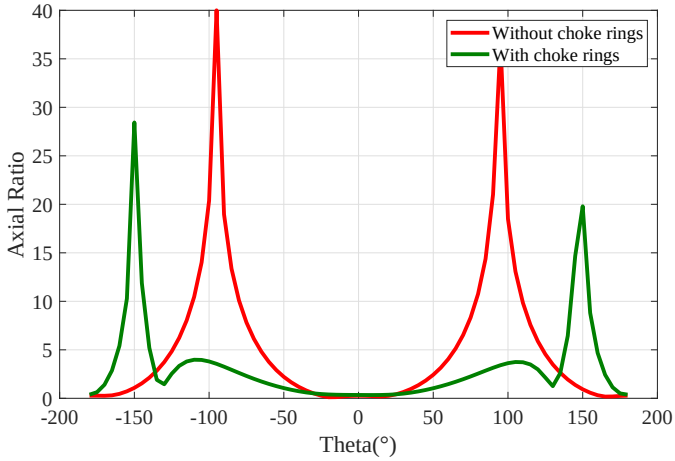

Fig. 9. Axial Ratio at E5a band.

spurious fields generated from the surface waves that traverse the substrate and are ultimately radiated from the ground and substrate truncations are therefore forced to travel these quarter-wavelength discs in opposite directions after being reflected from the metallic pillar. The electromagnetic currents travelling on the inner surface of these discs counterbalance themsleves out as discussed in Section III.

V. SIMULATION RESULTS

The proposed design was simulated in CST Microwave Studio 2019 [18] and the results are shown below.

Fig. 4 and Fig. 5 show the polar plots for the realized gain vs. the elevation angle θ, for both polarizations (RHCP and LHCP) in both bands (E1 and E5a) for both the design variations (one without the choke rings and one with the choke rings) at $\phi = 0°$. The realized gain obtained in the design with the choke rings was 6.5 dB compared to the 2.9 dB in the design without the choke rings for the E1 band while for the E5a band these values were 6 dB compared to 1.3 dB respectively. There was a drastic difference observed in the amplitude of the back lobe of the cross-polar (i.e. the LHCP) component as well. The details of all these and some other performance metrics are tabulated ahead.

For a better view towards the XPD performance, the co-polar and cross-polar components are plotted in Cartesian dimensions and are shown in Fig. 6 and Fig. 7, again for both bands. It is clearly visible that the design with the vertical choke rings not only suppresses the back lobe of the LHCP component, but also at elevation angles around the zenith until the entire horizon over the antenna ground plane, with the XPD ratio above 15 dB at very low elevation angles.

From Fig. 6 and Fig. 7, it is also seen that an FBR in excess of 25 dB and 20 dB is obtained for E1 band and E5a band respectively at $\phi = 0°$.

The axial ratio plots for the compared designs for both the bands are shown in Fig. 8 and Fig. 9. It can be seen that within the elevation beam sector above the horizon, the design with the choke rings perform much better with axial ratio below 3 in the entire angle span compared to the design without the choke rings that deteriorates fast beyond the $\pm 50°$ elevation span. As already talked about in section II-C of this paper and in [10], for the axial ratio to be good at angles close

TABLE I
ANTENNA PERFORMANCE METRICS

Parameters	**E1 Band**		**E5a Band**	
	Without choke rings	With choke rings	Without choke rings	With choke rings
Realized Gain (dB)	2,9	6,5	1,3	6,0
Axial Ratio @ $\theta = 75°$	5,4	1,0	8,3	2,2
Axial Ratio @ $\theta = 90°$	11,3	1,5	21,0	3,1
FBR (dB) @ $\phi = 0°$	4,0	26,1	1,4	19,5

to the horizon (i.e. around $\pm 90°$), there should be some co-polar radiation amplitude. From Fig. 6 and Fig. 7, we see that in both the bands of operation, the RHCP (co-polar) component is approximately 15 dB higher than the LHCP component at elevation angles approaching $\pm 90°$. On account of this significant difference in amplitude of the two orthogonal components, we obtain good axial ratios (< 3) at very low elevation angles as depicted in Fig. 8 and Fig. 9.

The important performance metrics are summarized in Table I. Apart from the values of the realized gain for both the bands that have been mentioned earlier, it is observed that the FBR values too are orders of magnitude higher for the design with the vertical choke rings.

For the axial ratio as well, both designs exhibit comparable values within a very small range in the vicinity of the zenith, but the deterioration in the design without the choke rings is very fast while it is notably stable in the improved design, namely 1,5 for the E1 band and 3,1 for the E5a band at elevations of $\pm 90°$.

VI. CONCLUSION

With the presented technique of designing vertical choke rings below the ground plane of a GNSS antenna, it has been shown that the back lobe of the cross-polar component can be remarkably reduced. This leads to a very high front-to-back ratio and the antenna is less susceptible to reflected signals coming from below the ground plane. This technique also allows the antenna to legibly retain its size and not become too bulky, as in the case of horizontally appended choke rings, along with keeping the design robust against manufacturing tolerances, unlike in the case of EBG structures on the RF substrate. This technique could be applied to novel conformal antenna arrays as in [19] and can be used in the deep analysis of interference in GNSS applications as in [20] for further improvement in multipath mitigation.

It is also observed that there is a good deal of co-polar radiation at the ground and substrate material truncations that leads to axial ratio values close to unity in the entire upper hemisphere, even at extremely low elevation angles ($\pm 90°$) which was also not achievable with horizontal choke rings since they abruptly terminate the surface current in the ground plane direction.

REFERENCES

[1] P. J. G. Teunissen, O. Montenbruck, *Springer Handbook of Global Navigation Satellite Systems*, 1989.

[2] E. D. Kaplan, C. Hegarty, *Understanding GPS/GNSS: Principles & Applications*, 3rd ed., 2017.

[3] D. Gebre-Egziabher, S. Gleason, *GNSS Applications & Methods*, 2009.

[4] M. Ibraheam et al., "Feasibility of dual-polarized antenna arrays for GNSS receivers at low elevations," *11th European Conference on Antennas and Propagation (EuCAP)*, Paris, 2017, pp. 857-861. doi: 10.23919/EuCAP.2017.7928441.

[5] M. Sgammini, S. Caizzone, A. Iliopoulos, A. Hornbostel, M. Meurer, "Interference mitigation using a dual-polarized antenna in a real environment," *Proceedings of the 29th International Technical Meeting of the Satellite Division of The Institute of Navigation (ION GNSS+ 2016)*, Portland, Oregon, September 2016, pp. 275-285.

[6] B. R. Rao, W. Kunysz, R. Fante, K. McDonald, *GPS/GNSS Antennas*, 2009.

[7] C. A. Balanis, *Antenna Theory: Analysis and Design*, Third Edition, 2012.

[8] S. Caizzone, M. -S. Circiu, W. Elmarissi, C. Enneking, M. Felux, K. Yinusa (2018), "Multipath rejection capability analysis of GNSS antennas", *ION GNSS+ 2018*, Miami, USA.

[9] D. R. Jackson, et al., "Microstrip patch designs that do not excite surface waves," *IEEE Trans. Ant. & Prop.*, Vol. 41 Is. 8, pp. 1026-1037, 1993.

[10] M. Maqsood, S. Gao, T. Brown and M. Unwin,"Effects of ground plane on the performance of multipath mitigating antennas for GNSS" *Antennas & Propagation Conference*, Loughborough, 2010, pp. 241-244. doi: 10.1109/ LAPC.2010.5666164.

[11] M. K. Emara, S. Gupta, J. S. Wight, J. Hautcoeur and G. Panther, "A low-profile dual-band tunable AMC structure for GNSS antennas and its performance trade-offs," *12th European Conference on Antennas and Propagation (EuCAP 2018)*, London, 2018, pp. 1-4.

[12] S. -S. Francesca, S. N. Makarov, "A Low Multipath Wideband GPS Antenna With Cutoff or Non-Cutoff Corrugated Ground Plane," *IEEE Transactions on Antennas and Propagation*, vol. 57 No. 1, pp. 3346, Jan. 2009.

[13] N. Ida, Chapter "Transmission Lines, Waveguides, and Resonant Cavities", In: *Microwave NDT. Developments in Electromagnetic Theory and Applications*, vol 10. Springer, Dordrecht (1992).

[14] R. E. Collin, *Electromagnetic Theory of Guided Waves*. NMcGraw-Hill (1991), NY, pp.564-568.

[15] MIT Opensource, "https://web.mit.edu/22.09/ClassHandouts/Charged%20Particle%20Accel/CHAP12.PDF".

[16] W. Kunysz, "A Three Dimensional Choke Ring Ground Plane Antenna.", Novatel Inc. (2003).

[17] Y. Lee, J. Yeo and R. Mittra, "Investigation of electromagnetic bandgap (EBG) structures for antenna pattern control," *IEEE Antennas and Propagation Society International Symposium*, Vol. 2, pp. 1115 1118, June, 2003.

[18] CST Microwave Studio, Version 2019.

[19] K. Yinusa, E. P. Marcos, S. Caizzone, (2018) "Robust Satellite Navigation by Means of a Spherical Cap Conformal Antenna Array". *18th International Symposium on Antenna Technology and Applied Electromagnetics*, 19.Aug. - 22.Aug.2018, Waterloo, ON, Canada.

[20] E. P. Marcos, A. Konovaltsev, S. Caizzone, M. Cuntz, K. Yinusa, W. Elmarissi, M. Meurer, "Interference and Spoofing Detection for GNSS Maritime Applications using Direction of Arrival and Conformal Antenna Array", In: *Proceedings of the 31st International Technical Meeting of the Satellite Division of the Institute of Navigation, ION GNSS+ 2018*, Miami, FL. Seiten 2907-2922.